

Universal scaling of strange particle p_T spectra in pp collisions

Liwen Yang, Yanyun Wang, Wenhui Hao, Na Liu, Xiaoling Du, and Wenchao Zhang

School of Physics and Information Technology, Shaanxi Normal University, Xi'an 710119, People's Republic of China
e-mail: wenchao.zhang@snnu.edu.cn

Received: date / Revised version: date

Abstract. As a complementary study to that performed on the transverse momentum (p_T) spectra of charged pions, kaons and protons in proton-proton (pp) collisions at LHC energies 0.9, 2.76 and 7 TeV, we present a scaling behaviour in the p_T spectra of strange particles (K_S^0 , Λ , Ξ and ϕ) at these three energies. This scaling behaviour is exhibited when the spectra are expressed in a suitable scaling variable $z = p_T/K$, where the scaling parameter K is determined by the quality factor method and increases with the center of mass energy (\sqrt{s}). The rates at which K increases with $\ln\sqrt{s}$ for these strange particles are found to be identical within errors. In the framework of the colour string percolation model, we argue that these strange particles are produced through the decay of clusters that are formed by the colour strings overlapping. We observe that the strange mesons and baryons are produced from clusters with different size distributions, while the strange mesons (baryons) K_S^0 and ϕ (Λ and Ξ) originate from clusters with the same size distributions. The cluster's size distributions for strange mesons are more dispersed than those for strange baryons. The scaling behaviour of the p_T spectra for these strange particles can be explained by the colour string percolation model in a quantitative way.

PACS. 13.85.Ni, 13.87.Fh

1 Introduction

The transverse momentum (p_T) spectra of final state particles are important observables in high energy collisions. They play an essential role in understanding the mechanism of particle productions. In many studies, searching for a scaling behaviour of the p_T spectra is useful to reveal the mechanism. In ref. [1], a scaling behaviour was presented in the pion p_T spectra in Au-Au collisions at the Relativistic Heavy Ion Collider (RHIC). It was independent of the centrality of the collision. This scaling behaviour was later extended to the proton and anti-proton p_T spectra with different centralities in Au-Au collisions at RHIC [2].

Recently, a similar scaling behaviour was found in the p_T spectra of inclusive charged hadrons as well as identified charged hadrons (charged pions, kaons and protons) in proton-proton (pp) collisions at the Large Hadron Collider (LHC) [3,4]. This scaling behaviour was independent of the center of mass energy (\sqrt{s}). It was exhibited when the spectra were expressed in a suitable scaling variable $z = p_T/K$, where K is the scaling parameter relying on \sqrt{s} . In pp collisions, the hadrons produced are predominantly pions, kaons and protons. As the strange quark is heavier than the up and down quarks, the strange particles such as K_S^0 , Λ , Ξ and ϕ only constitute a small fraction of final state particles. However, the investigation of their spectra is an important ingredient in understanding the mechanism of particle production in high energy collisions.

Thus, in this paper, we will focus on the p_T spectra of K_S^0 , Λ , Ξ and ϕ produced in pp collisions at 0.9, 2.76 and 7 TeV [5–10]. The p_T spectra of Ω are not considered in this work, as their spectra at 0.9 TeV are not available so far. A scaling behaviour independent of the collision energy will be searched for among these strange particle spectra. If the scaling behaviour exists, then one may ask two questions: (1) Is the dependence of the scaling parameter K on \sqrt{s} for K_S^0 , Λ , Ξ and ϕ the same as that for charged pions, kaons and protons? (2) Can the string percolation model utilized in ref. [4] be adopted to explain the scaling behaviour of strange particles?

The organization of the paper is as follows. In sect. 2, the method to search for the scaling behaviour will be described briefly. In sect. 3, the scaling behaviour of the K_S^0 , Λ , Ξ and ϕ spectra will be presented. In sect. 4, we will discuss the scaling behaviour of the strange particle spectra in the framework of the colour string percolation model. Finally, the conclusion is given in sect. 5.

2 Method to search for the scaling behaviour

As done in ref. [4], we will search for the scaling behaviour of the K_S^0 p_T spectra with the following steps. A scaling variable, $z = p_T/K$, and a scaled p_T spectrum, $\Phi(z) = A(2\pi p_T)^{-1} d^2N/dp_T dy|_{p_T=Kz}$ will be defined first. Here y is the rapidity of K_S^0 , $(2\pi p_T)^{-1} d^2N/dp_T dy$ is the invariant yield of K_S^0 . With suitable scaling parameters

K and A that depend on \sqrt{s} , the data points of the K_S^0 p_T spectra at 0.9, 2.76 and 7 TeV can be coalesced into one curve. In ref. [4], K and A for the charged pion, kaon and proton spectra at 2.76 TeV were set to be 1. This choice was made due to reason that the p_T coverage of the spectra at 2.76 TeV is much larger than the coverage at 0.9 and 2.76 TeV. In this work, the K_S^0 spectrum at 2.76 TeV covers a p_T range from 0.225 to 19 GeV/c, which is larger the ranges of the spectra at 0.9 and 7 TeV, 0.1 to 9 GeV/c and 0.1 to 9 GeV/c. Therefore, to keep the similarity and consistency with ref. [4], we prefer to set the K and A for the K_S^0 spectrum at 2.76 TeV to be 1. K and A values at 0.9 and 7 TeV will be determined by the quality factor method [11, 12]. Obviously, the scaling function $\Phi(z)$ depends on the choice of K and A at 2.76 TeV. This arbitrariness could be eliminated if the spectra are presented in $u = z/\langle z \rangle = p_T/\langle p_T \rangle$. Here $\langle z \rangle = \int_0^\infty z\Phi(z)zdz / \int_0^\infty \Phi(z)zdz$. The normalized scaling function then is $\Psi(u) = \langle z \rangle^2 \Phi(\langle z \rangle u) / \int_0^\infty \Phi(z)zdz$. With $\Psi(u)$, the spectra at 0.9 and 7 TeV can be parameterized as $f(p_T) = \int_0^\infty \Phi(z)zdz / (A\langle z \rangle^2 \Psi(p_T/(K\langle z \rangle)))$, where K and A are the scaling parameters at these energies. The methods to search for the scaling behaviour of the Λ , Ξ and ϕ spectra are similar to that for the K_S^0 spectra.

3 Scaling behaviour of the K_S^0 , Λ , Ξ and ϕ p_T spectra

The K_S^0 , Λ and Ξ p_T spectra in pp collisions at 0.9 and 7 TeV were published by the CMS collaboration [5]. Here Λ and Ξ refer to $(\Lambda + \bar{\Lambda})/2$ and $(\Xi^+ + \Xi^-)/2$ respectively. For the K_S^0 , Λ and Ξ p_T spectra at 2.76 TeV, so far there are no official data. As the K_S^0 spectrum is theoretically the same as the charged kaon spectrum, and the charged kaon spectrum at 2.76 TeV were officially published in ref. [13], we utilize the charged kaon spectrum instead of the K_S^0 spectrum at this energy. For the Λ and Ξ spectra at 2.76 TeV, we use the preliminary results of the ALICE collaboration at this energy instead. They are publicly available in refs. [6, 7]. The ϕ spectra at 0.9, 2.76 and 7 TeV were published by the ALICE collaboration [8–10]. Since the scaling parameters K and A at 2.76 TeV are chosen to be 1, the scaling function $\Phi(z)$ is exactly the K_S^0 , Λ , Ξ or ϕ p_T spectrum at this energy. As described in ref. [14], due to the reason that the temperature of the hadronizing system fluctuates from event to event, the p_T spectrum of final state hadrons produced in high energy collisions follows a non-extensive statistical distribution, the Tsallis distribution [15]. Thus, the scaling function $\Phi(z)$ for strange particles can be parameterized as follows [4]

$$\Phi(z) = C_q \left[1 - (1 - q) \frac{\sqrt{m^2 + z^2} - m}{z_0} \right]^{\frac{1}{1-q}}, \quad (1)$$

where C_q , q and z_0 are free parameters, $1 - q$ is a measure of the non-extensivity, m is the strange particle mass. In eq. (1), $1/(q - 1)$ determines the power law behaviour of

$\Phi(z)$ in the high p_T region, while z_0 controls the exponential behaviour in the low p_T region. C_q , q and z_0 are determined by the least squares fitting of $\Phi(z)$ to the K_S^0 , Λ , Ξ and ϕ p_T spectra at 2.76 TeV. The statistical and systematic errors of the data points have been added in quadrature in the fits. Table 1 tabulates C_q , q , z_0 and their uncertainties returned by the fits. The χ^2 s per degrees of freedom (dof), named reduced χ^2 s, for these fits are also given in the table.

Table 1. C_q , q and z_0 of $\Phi(z)$ for the K_S^0 , Λ , Ξ and ϕ spectra. The uncertainties quoted are due to the quadratic sum of the statistical and systematic errors of the data points. The last column shows the reduced χ^2 s for the fits on the strange p_T spectra at 2.76 TeV.

	C_q	q	z_0 (GeV/c)	χ^2/dof
K_S^0	$(214 \pm 2) \times 10^{-3}$	1.1402 ± 0.0004	0.193 ± 0.001	12.91/55
Λ	$(21 \pm 1) \times 10^{-3}$	1.106 ± 0.005	0.260 ± 0.008	6.63/26
Ξ	$(169 \pm 3) \times 10^{-5}$	1.104 ± 0.003	0.300 ± 0.004	3.28/11
ϕ	$(96 \pm 4) \times 10^{-4}$	1.141 ± 0.004	0.263 ± 0.007	6.25/18

As described in sect. 2, the scaling parameters K and A at 0.9 and 7 TeV will be evaluated with the quality factor (QF) method. Compared with the method utilized in ref. [3], this method is more robust since it does not rely on the shape of the scaling function. To define the quality factor, a set of data points (ρ^i, τ^i) is considered first. Here $\rho^i = p_T^i/K$, $\tau^i = \log(A(2\pi p_T^i)^{-1} d^2 N^i / dp_T^i dy^i)$, ρ^i are ordered, τ^i are rescaled so that they are in the range between 0 and 1. Then, the QF is introduced as follows [11, 12]

$$\text{QF}(K, A) = \left[\sum_{i=2}^n \frac{(\tau^i - \tau^{i-1})^2}{(\rho^i - \rho^{i-1})^2 + 1/n^2} \right]^{-1}, \quad (2)$$

where n is the number of data points and $1/n^2$ keeps the sum finite in the case of two points taking the same ρ value. It is obvious that a large contribution to the sum in the QF is given if two successive data points are close in ρ and far in τ . Therefore, a set of data points are expected to lie close to a single curve if they have a small sum (a large QF) in eq. (2). The best set of (K, A) at 0.9 (7) TeV is chosen to be the one which globally maximizes the QF of the data points at 0.9 (7) and 2.76 TeV. Table 2 tabulates K and A for the K_S^0 , Λ , Ξ and ϕ spectra at 0.9, 2.76 and 7 TeV. Also shown in the table is the maximum QF (QF_{max}). In order to determine the uncertainties of K and A at 0.9 and 7 TeV, we utilize the method mentioned in ref. [11]. Let's take the determination of the uncertainty of K (A) for K_S^0 at 0.9 TeV as an example. In fig. 1 we first plot the QF as a function of K (A) with A (K) fixed to the value 0.24 (0.92) returned by the QF method. The peak value with $\text{QF} > (\text{QF}_{\text{max}} - 0.01)$ shows a good scaling and we make a Gaussian fit to this bump. The standard deviation of the Gaussian fit, $\sigma_{K(A)}$, is taken as the uncertainty of K (A) for K_S^0 at 0.9 TeV. The mean value of the Gaussian fit, $\mu_{K(A)}$, is consistent with the value of K

(A) returned by the QF method, thus this method to determine the uncertainties of scaling parameters is robust. The errors of K and A for K_S^0 at 7 TeV, Λ , Ξ and ϕ at 0.9 and 7 TeV are determined by making Gaussian fits to the peaks with $QF > (QF_{\max} - 0.01)$.

Table 2. K and A for the K_S^0 , Λ , Ξ and ϕ spectra at 0.9, 2.76 and 7 TeV. The QF_{\max} is shown in the last column of the table. The standard deviations of the Gaussian fits to the peaks of the QF scatter plots at 0.9 and 7 TeV are taken as the uncertainties of K and A at these two energies.

	\sqrt{s} (TeV)	K	A	QF_{\max}
K_S^0	0.9	0.92 ± 0.01	0.24 ± 0.02	0.92
	2.76	1	1	-
	7	1.14 ± 0.01	0.23 ± 0.02	0.92
Λ	0.9	0.85 ± 0.01	0.20 ± 0.02	1.46
	2.76	1	1	-
	7	1.10 ± 0.02	0.20 ± 0.02	1.21
Ξ	0.9	0.86 ± 0.02	0.20 ± 0.03	1.94
	2.76	1	1	-
	7	1.13 ± 0.02	0.20 ± 0.02	2.16
ϕ	0.9	0.85 ± 0.06	0.89 ± 0.17	6.96
	2.76	1	1	-
	7	1.06 ± 0.03	0.91 ± 0.07	2.89

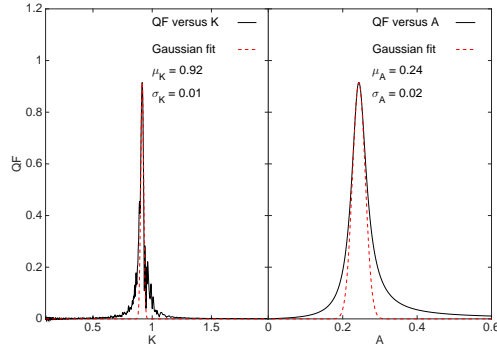


Fig. 1. Left (right) panel: QF versus K (A) for K_S^0 at 0.9 TeV, with A (K) fixed to 0.24 (0.92). The black solid curve is the QF scatter plot, the red dash curve is the Gaussian fit of the peak with $QF > 0.91$.

Using the scaling parameters K and A in table 2, now we can shift the K_S^0 p_T spectra at 0.9 and 7 TeV to the spectrum at 2.76 TeV. They are shown in the upper panel of fig. 2. On a log scale, most of the data points at different energies appear consistent with the universal curve which is described by $\Phi(z)$ in eq. (1) with parameters in the second row of table 1. In order to see how well the data points agree with the fitted curve, a ratio, $R = (\text{data} - \text{fitted})/\text{data}$, is evaluated at 0.9, 2.76 and 7 TeV. The uncertainty of R is determined to be $(\text{fitted}/\text{data}) \times (\Delta\text{data}/\text{data})$, where Δdata is the total uncertainty of the data point. The R distribution is shown

in the lower panel of the figure. Except for the last three points in the high p_T region at 0.9 TeV, all the other points have R values in the range between -0.3 and 0.3, which implies that the agreement between the data points and the fitted curve is within 30%. This agreement roughly corresponds to the systematic errors on R and the accuracy of the fits. If we take into account the systematic errors on R , then this agreement is within 22%.

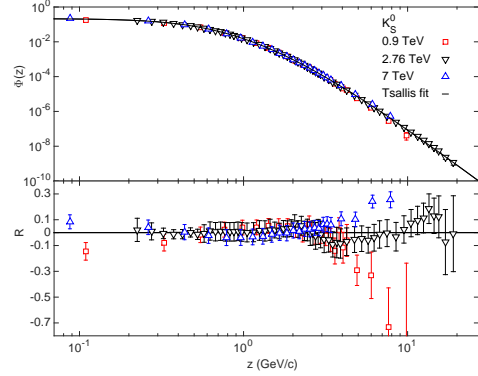


Fig. 2. Upper panel: the scaling behaviour of the K_S^0 p_T spectra presented in z at 0.9, 2.76 and 7 TeV. The solid curve is from $\Phi(z)$ with parameters in the second row of table 1. The data points are taken from refs. [5,13]. Lower panel: the R distributions. The R value for the last data point at 0.9 TeV is -1.27 and it is not shown in the lower panel.

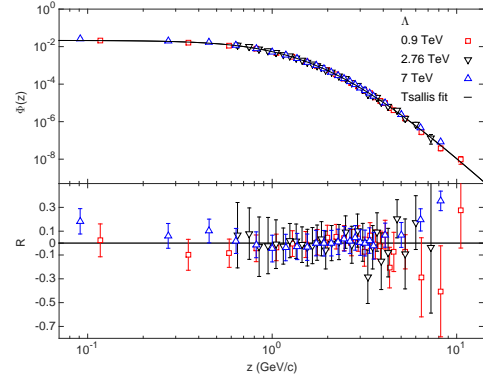


Fig. 3. Upper panel: the scaling behaviour of the Λ p_T spectra presented in z at 0.9, 2.76 and 7 TeV. The solid curve is from $\Phi(z)$ with parameters in the third row of table 1. The data points are taken from refs. [5,6]. Lower panel: the R distributions.

In the upper panels of figs. 3, 4 and 5, we present the scaling behaviour of the Λ , Ξ and ϕ p_T spectra at 0.9, 2.76 and 7 TeV. In the lower panels of these figures are the R distributions for these spectra. For the Λ spectra, except for the second-to-last point at 0.9 TeV and the last point at 7 TeV, all the other points agree with the fitted curve within 30%. Taking into account the systematic uncertainties of R , this agreement is within 11%. For the Ξ spectra,

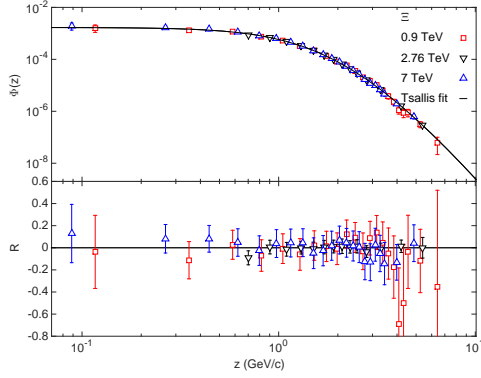


Fig. 4. Upper panel: the scaling behaviour of the Ξ p_T spectra presented in z at 0.9, 2.76 and 7 TeV. The solid curve is from $\Phi(z)$ with parameters in the fourth row of table 1. The data points are taken from refs. [5, 7]. Lower panel: the R distributions.

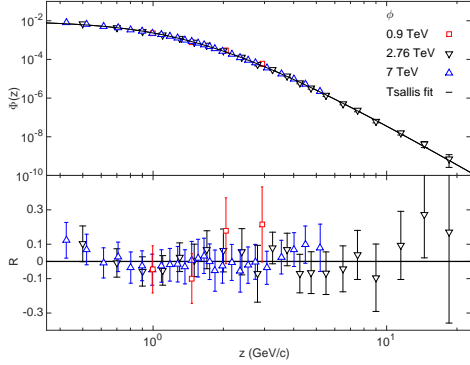


Fig. 5. Upper panel: the scaling behaviour of the ϕ p_T spectra presented in z at 0.9, 2.76 and 7 TeV. The solid curve is from $\Phi(z)$ with parameters in the fifth row of table 1. The data points are taken from refs. [8–10]. Lower panel: the R distributions.

except for the points with $z = 4.1, 4.3$ and 6.4 GeV/c at 0.9 TeV, all the other points are consistent with the fitted curve within 20%. Taking into account the systematic errors of R , this consistency is within 3%. For the ϕ spectra, all the points are in agreement with the fitted curve within 30%. With the consideration of the systematic errors of R , this agreement is within 18%.

From the above statement, we have shown that the p_T spectra of K_S^0 , Λ , Ξ and ϕ at 0.9, 2.76 and 7 TeV exhibit a scaling behaviour independent of \sqrt{s} . As described in sect. 2, the scaling function $\Phi(z)$ relies on K and A chosen at 2.76 TeV. In order to get rid of this reliance, we utilize the scaling variable $u = z/\langle z \rangle$ instead. The $\langle z \rangle$ values for the K_S^0 , Λ , Ξ and ϕ p_T spectra are determined as 0.701 ± 0.008 , 0.97 ± 0.03 , 1.12 ± 0.01 and 1.04 ± 0.02 GeV/c, where the errors are due to the uncertainties of C_q , q and z_0 in table 1. The corresponding normalized scaling function $\Psi(u)$ is

$$\Psi(u) = C'_q \left[1 - (1 - q') \frac{\sqrt{(m')^2 + u^2} - m'}{u_0} \right]^{\frac{1}{1-q'}}. \quad (3)$$

Here $C'_q = \langle z \rangle^2 C_q / \int_0^\infty \Phi(z) z dz$, $q' = q$, $u_0 = z_0 / \langle z \rangle$ and $m' = m / \langle z \rangle$. Their values are presented in table 3. As described in sect. 2, with $\Psi(u)$, the spectra of K_S^0 , Λ , Ξ and ϕ at 0.9 (7) TeV can be parameterized as $f(p_T) = \int_0^\infty \Phi(z) z dz / (A \langle z \rangle^2) \Psi(p_T / (K \langle z \rangle))$, where K and A are the scaling parameters of these strange particles at 0.9 (7) TeV in table 2. In ref. [5], the CMS collaboration have presented the relative production versus p_T between different strange particle species, $N(\Lambda)/N(K_S^0)$ and $N(\Xi)/N(\Lambda)$, at 0.9 and 7 TeV. In the upper (lower) panel of fig. 6, we show that the $N(\Lambda)/N(K_S^0)$ ($N(\Xi)/N(\Lambda)$) distributions in data at 0.9 and 7 TeV are well described by $f_\Lambda(p_T)/f_{K_S^0}(p_T)$ ($f_\Xi(p_T)/f_\Lambda(p_T)$). This agreement is a definite indication that the scaling behaviour exists in the p_T spectra of strange particles at 0.9, 2.76 and 7 TeV. The p_T dependence of the relative production can be explained as follows. At low p_T , $f(p_T)$ inclines to be an exponential distribution which is controlled by the parameter $z_0 = u_0 \langle z \rangle$. For $N(\Lambda)/N(K_S^0)$ ($N(\Xi)/N(\Lambda)$), the z_0 value for Λ (Ξ) is larger than that for K_S^0 (Λ), therefore both $N(\Lambda)/N(K_S^0)$ and $N(\Xi)/N(\Lambda)$ grow with p_T . At high p_T , $f(p_T)$ prefers to be a power law distribution which is dominated by $1/(q' - 1)$. q' value for Λ (Ξ) is smaller than (almost equal to) that for K_S^0 (Λ), thus $N(\Lambda)/N(K_S^0)$ decreases with p_T while $N(\Xi)/N(\Lambda)$ appears to be flat.

Table 3. C'_q , q' , u_0 and m' of $\Psi(u)$ for K_S^0 , Λ , Ξ and ϕ . The uncertainties quoted are due to the errors of C_q , q and z_0 in table 1.

	C'_q	q'	u_0	m'
K_S^0	2.86 ± 0.03	1.1402 ± 0.0004	0.275 ± 0.004	0.704 ± 0.008
Λ	2.23 ± 0.04	1.106 ± 0.005	0.268 ± 0.004	1.15 ± 0.03
Ξ	2.21 ± 0.02	1.104 ± 0.003	0.267 ± 0.002	1.32 ± 0.01
ϕ	2.54 ± 0.04	1.141 ± 0.004	0.254 ± 0.003	0.98 ± 0.02

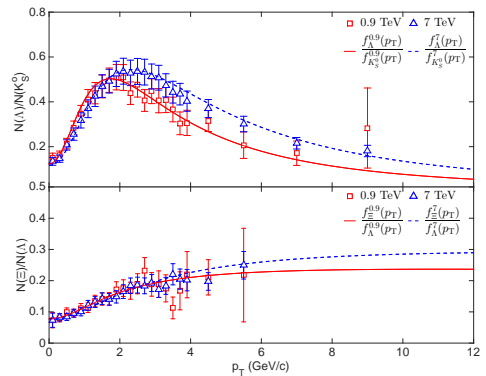


Fig. 6. Upper (Lower) panel: the $N(\Lambda)/N(K_S^0)$ ($N(\Xi)/N(\Lambda)$) distributions at 0.9 (solid line) and 7 TeV (dashed line). The data points are taken from ref. [5]. The values of $N(\Lambda)/N(K_S^0)$ for data points have been divided by 2, since here Λ refers to $(\Lambda + \bar{\Lambda})/2$.

4 Discussions

In sect. 3, we have shown that there is indeed a scaling behaviour in the K_S^0 , Λ , Ξ and ϕ p_T spectra in pp collisions at 0.9, 2.76 and 7 TeV. This scaling behaviour appears when the spectra are presented in terms of the scaling variable z . Now we would like to discuss this scaling behaviour in terms of the colour string percolation (CSP) model [16, 17].

In this model, colour strings are stretched between the partons of the projectile and target protons in pp collisions. These strings then will split into new ones by the production of sea $q\bar{q}$ pairs from the vacuum. Strange particles such as K_S^0 , Λ , Ξ and ϕ are produced through the hadronization of these new strings. In the transverse plane, the colour strings look like discs, each of which has an area, $S_1 = \pi r_0^2$, $r_0 \approx 0.2$ fm. When the collision energy increases, the number of strings grows and they interact with each other and start to overlap to form clusters. A cluster with n strings is assumed to behave as a single string. The colour field of the cluster \vec{Q}_n is the vectorial sum of the colour charge of each individual \vec{Q}_1 string, $\vec{Q}_n = \sum_1^n \vec{Q}_1$. Since the individual string colour fields are oriented arbitrarily, the average value of $\vec{Q}_{1i} \cdot \vec{Q}_{1j}$ is zero and $\vec{Q}_n^2 = n\vec{Q}_1^2$. \vec{Q}_n also depends on the transverse area of each individual string S_1 and the transverse area of the cluster S_n . Thus, $Q_n = \sqrt{nS_n/S_1}Q_1$. As the multiplicity of strange particles produced from the cluster is proportional to its colour charge, $\mu_n = \sqrt{nS_n/S_1}\mu_1$, where μ_1 is the multiplicity of strange particles produced by a single string. Since the transverse momentum is conserved before and after the overlapping, $\mu_n \langle p_T^2 \rangle_n = n\mu_1 \langle p_T^2 \rangle_1$, where $\langle p_T^2 \rangle_n$ is the mean p_T^2 of strange particles produced by the cluster, $\langle p_T^2 \rangle_1$ is the mean p_T^2 of strange particles produced by a single string. Therefore, $\langle p_T^2 \rangle_n = \sqrt{nS_1/S_n} \langle p_T^2 \rangle_1$, where nS_1/S_n is the degree of string overlap. For the case where strings just get in touch with each other, $S_n = nS_1$, $nS_1/S_n = 1$ and $\langle p_T^2 \rangle_n = \langle p_T^2 \rangle_1$, which means that the n strings fragment into strange hadrons independently. For the case in which strings maximally overlap with each other, $S_n = S_1$, $nS_1/S_n = n$ and $\langle p_T^2 \rangle_n = \sqrt{n} \langle p_T^2 \rangle_1$, which means that the mean p_T^2 is maximally enhanced due to the percolation. The p_T spectra of strange particles produced in pp collisions can be written as a superposition of the p_T distribution produced by each cluster, $g(x, p_T)$, weighted with the cluster's size distribution $W(x)$,

$$\frac{d^2N}{2\pi p_T dp_T dy} = C \int_0^\infty W(x) g(x, p_T) dx, \quad (4)$$

where C is a normalization parameter which characterizes the total number of clusters formed for strange particles before hadronization. $W(x)$ is supposed to be a gamma distribution,

$$W(x) = \frac{\gamma}{\Gamma(\kappa)} (\gamma x)^{\kappa-1} \exp(-\gamma x), \quad (5)$$

where x is proportional to $1/\langle p_T^2 \rangle_n$, κ and γ are free parameters. κ is related to the dispersion of the size distribution, $1/\kappa = (\langle x^2 \rangle - \langle x \rangle^2)/\langle x \rangle^2$. It depends on the density

of the strings, $\eta = (r_0/R)^2 N_s$, where R is the effective radius of the interaction region, N_s is the average number of strings of the cluster. γ is related to the mean x , $\langle x \rangle = \kappa/\gamma$.

In order to see whether the CSP model can describe the scaling behaviour of strange particle p_T spectra, we attempt to fit eq. (4) to the combination of the scaled data points at 0.9, 2.76 and 7 TeV with the least squares method. Here the cluster's fragmentation function in the CSP fit is chosen as the Schwinger formula [18]

$$g(x, p_T) = \exp(-p_T^2 x). \quad (6)$$

C , γ and κ returned by the fits are listed in table 4. From the table, we see that the dispersion of the cluster's size distribution ($1/\kappa$) for strange mesons (K_S^0 and ϕ) is larger than that of strange baryons (Λ and Ξ), while the dispersion of the cluster's size distribution for K_S^0 (Λ) is almost equal to that of ϕ (Ξ) when considering the errors. This implies that the strange mesons and baryons are produced from clusters with different size distributions, while the strange mesons (baryons) K_S^0 and ϕ (Λ and Ξ) originate from clusters with the same size distributions. The cluster's size distributions for strange mesons are more dispersed than those for strange baryons. The difference between the cluster's size distributions of strange mesons and baryons could be explained as follows. As described in ref. [16], since additional quarks required to form a baryon are provided by the quarks of the overlapping strings that form the cluster, the baryons probe a higher string density than mesons for the same energy of collisions. When η is above the critical string density at which the string percolation appears, κ increases with η [19]. Therefore the κ values for strange baryons are larger than those for strange mesons. The fit results for K_S^0 , Λ , Ξ and ϕ are presented in the upper panels of figs. 7, 8, 9 and 10 respectively. The R distributions are shown in the lower panels of these figures. For the K_S^0 spectra, except for the last two points at 0.9 TeV and the last three points at 2.76 TeV, all the other points agree with the CSP fit within 30%. For the Λ spectra, except for the points with $z = 6.4$ and 8.2 GeV/c at 0.9 TeV, all the other data points are consistent with the CSP fit within 30%. For the Ξ spectra, except for the points at $z = 4.1$, 4.3 and 6.4 GeV/c at 0.9 TeV, all the other data points agree with the CSP fit within 20%. For the ϕ spectra, except for the last point at 2.76 TeV, all the other points are consistent with the CSP fit within 30%.

Table 4. C , γ and κ returned by the CSP fits on the combination of the scaled K_S^0 , Λ , Ξ and ϕ spectra at 0.9, 2.76 and 7 TeV. The uncertainties quoted originate from the statistical and systematic errors of the data points added in quadrature. The last column shows the reduced χ^2 s for the fits.

	C	γ	κ	χ^2/dof
K_S^0	$(166 \pm 4) \times 10^{-3}$	0.89 ± 0.02	3.04 ± 0.02	272.50/103
Λ	$(197 \pm 5) \times 10^{-4}$	2.54 ± 0.07	3.80 ± 0.04	37.31/74
Ξ	$(155 \pm 4) \times 10^{-4}$	3.44 ± 0.11	3.83 ± 0.05	18.86/55
ϕ	$(86 \pm 3) \times 10^{-4}$	1.94 ± 0.06	3.09 ± 0.03	20.27/48

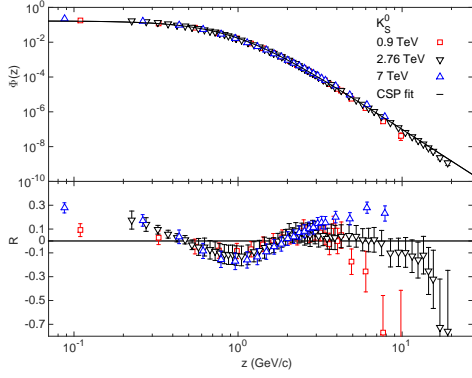


Fig. 7. Upper panel: the scaling behaviour of the K_S^0 p_T spectra presented in z at 0.9, 2.76 and 7 TeV. The solid curve is the CSP fit in eq. (4) with parameters in the second row of table 4. The data points are taken from refs. [5, 13]. Lower panel: the R distributions. The R value for the last data point at 0.9 TeV is -1.60 and it is not shown in the lower panel.

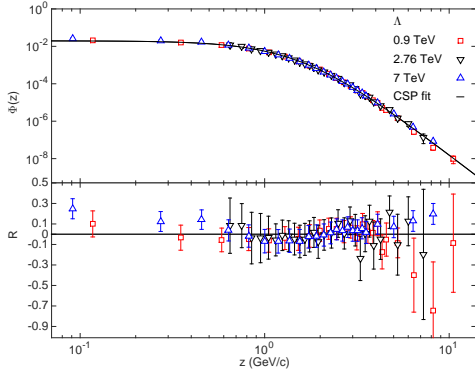


Fig. 8. Upper panel: the scaling behaviour of the Λ p_T spectra presented in z at 0.9, 2.76 and 7 TeV. The solid curve is the CSP fit in eq. (4) with parameters in the third row of table 4. The data points are taken from refs. [5, 6]. Lower panel: the R distributions.

From the above statement, we see that the CSP model can successfully describe the scaling behaviour of the strange particle p_T spectra at 0.9, 2.76 and 7 TeV. The reason is as follows. $W(x)$ in eq. (5) and $g(x, p_T)$ in eq. (6) are invariant under the transformation $x \rightarrow x' = \lambda x$, $\gamma \rightarrow \gamma' = \gamma/\lambda$ and $p_T \rightarrow p'_T = p_T/\sqrt{\lambda}$. Here $\lambda = \langle S_n/nS_1 \rangle^{1/2}$, where the average is taken over all the clusters decaying into strange particles [17]. As a result, the strange particle p_T spectra in eq. (4) are also invariant. This invariance is exactly the scaling behaviour we are looking for. Comparing the p'_T transformation in the CSP model $p'_T \rightarrow p'_T\sqrt{\lambda}$ with the one utilized to search for the scaling behaviour $p_T \rightarrow p_T/K$, we deduce that the scaling parameter K is proportional to $\langle nS_1/S_n \rangle^{1/4}$. As the degree of string overlap nS_1/S_n nonlinearly grows with \sqrt{s} [16, 19], the scaling parameter K should also increase with \sqrt{s} in a nonlinear trend. That's indeed what we observed in table 2. There-

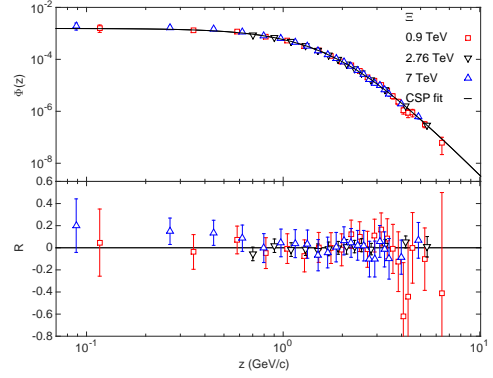


Fig. 9. Upper panel: the scaling behaviour of the Ξ p_T spectra presented in z at 0.9, 2.76 and 7 TeV. The solid curve is the CSP fit in eq. (4) with parameters in the fourth row of table 4. The data points are taken from refs. [5, 7]. Lower panel: the R distributions.

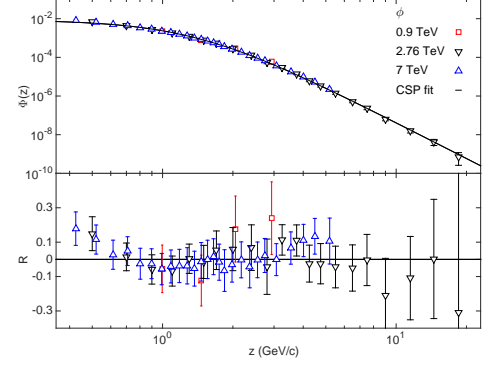


Fig. 10. Upper panel: the scaling behaviour of the ϕ p_T spectra presented in z at 0.9, 2.76 and 7 TeV. The solid curve is the CSP fit in eq. (4) with parameters in the fifth row of table 4. The data points are taken from refs. [8–10]. Lower panel: the R distributions.

fore the CSP model can qualitatively explain the scaling behaviour for the K_S^0 , Λ , Ξ and ϕ p_T spectra separately.

In order to determine the nonlinear trend with which K increases with \sqrt{s} , we fit the K values at 0.9, 2.76 and 7 TeV for K_S^0 , Λ , Ξ and ϕ in table 2 with a function $K = \alpha \ln(\sqrt{s}) + \beta$, where \sqrt{s} is in TeV, α and β are free parameters and α characterizes the rate at which K changes with $\ln\sqrt{s}$. In sect. 2, the scaling parameter K at 2.76 TeV is set to be 1 and it is not assigned to an uncertainty. Here, in order to do the fit, we take its uncertainty as the relative error of $\langle p_T \rangle$ at this energy. The α values returned by the fits for K_S^0 , Λ , Ξ and ϕ are 0.109 ± 0.024 , 0.120 ± 0.028 , 0.131 ± 0.031 and 0.085 ± 0.026 . They are consistent within uncertainties. This can be explained by the CSP model as follows. The values of $\langle z \rangle$ are the same for K_S^0 (Λ , Ξ or ϕ) at 0.9, 2.76 and 7 TeV. As $K = \langle p_T \rangle / \langle z \rangle$, the ratio between the values of K should be equal to the ratio between the values of $\langle p_T \rangle$. $\langle p_T \rangle$ is evaluated in terms of the

CSP model as [4]

$$\langle p_T \rangle = \frac{\int_0^\infty \int_0^\infty W(x)g(x, p_T)p_T^2 dx dp_T}{\int_0^\infty \int_0^\infty W(x)g(x, p_T)p_T dx dp_T}. \quad (7)$$

Plugging $W(x)$ in eq. (5) and $g(x, p_T)$ in eq. (6) into eq. (7), we get

$$\langle p_T \rangle = \frac{\sqrt{\gamma\pi}(\kappa - 1)\Gamma(\kappa - \frac{3}{2})}{2\Gamma(\kappa)}, \quad (8)$$

which depends on γ and κ . In order to determine the values of γ and κ at 0.9, 2.76 and 7 TeV, we fit the strange particle spectra at these three energies to eq. (4) with the least squares method. They are tabulated in table 5. With these γ and κ values, we can calculate the ratios between the values of $\langle p_T \rangle$ at 0.9 (7) and 2.76 TeV for K_S^0 , Λ , Ξ and ϕ . They are 0.93 ± 0.03 , 0.87 ± 0.04 , 0.86 ± 0.04 and 0.95 ± 0.38 (1.14 ± 0.03 , 1.08 ± 0.04 , 1.08 ± 0.04 and 1.03 ± 0.03), where uncertainties are due to the errors of γ and κ at 0.9 (7) and 2.76 TeV. Comparing these ratios with the scaling parameters K at 0.9 and 7 TeV in table 2, we find they are indeed consistent within uncertainties. Therefore, the CSP model can also explain the scaling behaviour of the K_S^0 , Λ , Ξ and ϕ p_T spectra in a quantitative way.

Finally, we would like to see whether the energy dependence of the scaling parameter K for the strange particles K_S^0 , Λ , Ξ and ϕ is the same as that for charged pions, kaons and protons. We fit $K = \alpha \ln(\sqrt{s}) + \beta$ to the K values at 0.9, 2.76 and 7 TeV for charged pions, kaons and protons in ref. [4]. The values of α for charged pions, kaons and protons are 0.0638 ± 0.0008 , 0.085 ± 0.015 and 0.088 ± 0.003 . The α value for charged pions is smaller than those for the strange particles while the α values for charged kaons and protons are comparable to those for the strange particles.

Table 5. C , γ and κ returned by the CSP fits on the K_S^0 , Λ , Ξ and ϕ spectra at 0.9, 2.76 and 7 TeV. The uncertainties quoted originate from the statistical and systematic errors of the data points added in quadrature. The last column shows the reduced χ^2 s for the fits.

	$\sqrt{s}(\text{TeV})$	C	γ	κ	χ^2/dof
K_S^0	0.9	$(64 \pm 4) \times 10^{-2}$	0.83 ± 0.05	3.13 ± 0.06	45.08/21
	2.76	$(166 \pm 4) \times 10^{-3}$	0.91 ± 0.02	3.06 ± 0.02	70.61/55
	7	$(79 \pm 4) \times 10^{-2}$	0.95 ± 0.05	2.80 ± 0.03	42.34/21
Λ	0.9	$(90 \pm 4) \times 10^{-3}$	2.14 ± 0.10	4.02 ± 0.07	8.55/21
	2.76	$(19 \pm 2) \times 10^{-3}$	2.57 ± 0.18	3.80 ± 0.09	6.53/26
	7	$(108 \pm 4) \times 10^{-3}$	2.76 ± 0.09	3.64 ± 0.04	6.26/21
Ξ	0.9	$(72 \pm 4) \times 10^{-4}$	2.95 ± 0.27	4.12 ± 0.18	7.84/19
	2.76	$(148 \pm 3) \times 10^{-5}$	3.52 ± 0.10	3.82 ± 0.05	1.37/11
	7	$(89 \pm 3) \times 10^{-4}$	3.88 ± 0.23	3.69 ± 0.10	3.25/19
ϕ	0.9	$(152 \pm 9) \times 10^{-3}$	0.53 ± 0.41	2.09 ± 0.44	0.56/1
	2.76	$(78 \pm 3) \times 10^{-4}$	2.15 ± 0.11	3.18 ± 0.04	7.30/18
	7	$(102 \pm 3) \times 10^{-4}$	1.83 ± 0.06	2.89 ± 0.03	3.64/23

5 Conclusions

In this paper, we have presented the scaling behaviour of the K_S^0 , Λ , Ξ p_T and ϕ p_T spectra at 0.9, 2.76 and 7 TeV. This scaling behaviour appears when the spectra are shown in terms of the scaling variable $z = p_T/K$. The scaling parameter K is determined by the quality factor method and it increases with energy. The rates at which K increases with $\ln\sqrt{s}$ for these strange particles are found to be identical within errors. In the framework of the CSP model, the strange particles are produced through the decay of clusters that are formed by the strings overlapping. We find that the strange mesons and baryons are produced from clusters with different size distributions, while the strange mesons (baryons) K_S^0 and ϕ (Λ and Ξ) originate from clusters with the same size distributions. The cluster's size distributions for strange mesons are more dispersed than those for strange baryons. The scaling behaviour of the p_T spectra for these strange particles can be explained by the colour string percolation model quantitatively.

Acknowledgements

Liwen Yang, Yanyun Wang, Na Liu, Xiaoling Du and Wenchao Zhang were supported by the Fundamental Research Funds for the Central Universities of China under Grant No. GK201502006, by the Scientific Research Foundation for the Returned Overseas Chinese Scholars, State Education Ministry, by Natural Science Basic Research Plan in Shaanxi Province of China under Grant No. 2017JM1040, and by the National Natural Science Foundation of China under Grant Nos. 11447024 and 11505108. Wenhui Hao was supported by the National Student's Platform for Innovation and Entrepreneurship Training Program under Grant No. 201710718043.

References

1. R. C. Hwa and C. B. Yang, Phys. Rev. Lett. **90**, 212301 (2003).
2. W. C. Zhang, Y. Zeng, W. X. Nie, L. L. Zhu and C. B. Yang, Phys. Rev. C **76**, 044910 (2007).
3. W. C. Zhang and C. B. Yang, J. Phys. G: Nucl. Part. Phys. **41**, 105006 (2014).
4. W. C. Zhang, J. Phys. G: Nucl. Part. Phys. **43**, 015003 (2016).
5. V. Khachatryan et al. (CMS Collaboration), J. High Energy Phys. **05**, 064 (2011).
6. L. D. Hanratty, CERN-THESIS-2014-103 (2014).
7. D. Colella (for the ALICE Collaboration), J. Phys.: Conf. Ser. **509**, 012090 (2014).
8. K. Aamodt et al. (ALICE Collaboration), Eur. Phys. J. C **71**, 1594 (2011).
9. J. Adam et al. (ALICE Collaboration), Phys. Rev. C **95**, 064606 (2017).
10. B. Abelev et al. (ALICE Collaboration), Eur. Phys. J. C **72**, 2183 (2012).

11. F. Gelis et al., Phys. Lett. B **647**, 376-379 (2007).
12. G. Beuf et al., Phys. Rev. D **78**, 074004 (2008).
13. B. Abelev et al. (ALICE Collaboration), Phys. Lett. B **736**, 196-207 (2014).
14. M. Rybczynski, Z. Wlodarczyk and G. Wilk, J. Phys. G: Nucl. Part. Phys. **39**, 095004 (2012).
15. C. Tsallis, J. Stat. Phys. **52**, 479 (1988).
16. L. Cunqueiro et al., Eur. Phys. J. C **53**, 585-589 (2008).
17. J. Dias de Deus et al., Eur. Phys. J. C **41**, 229-241 (2005).
18. J. Schwinger, Phys. Rev. **82**, 664 (1951).
19. J. Dias de Deus et al., Phys. Lett. B **601**, 125-131 (2004).